Electroretinogram Analysis In Patients With Non-Proliferative Diabetic Retinopathy

Zahra Maleki
Islamic Azad University
Soroor Behbahani (sor.behbahani@gmail.com)
Islamic Azad University
Hamid Ahmadieh
Shahid Beheshti University of Medical Sciences

Research Article

Keywords: Diabetic retinopathy, Electroretinogram, Theta angle criterion, Parabolic mapping, Retina

Posted Date: December 10th, 2021

DOI: https://doi.org/10.21203/rs.3.rs-827244/v1

Abstract

Purpose: Non-proliferative diabetic retinopathy (NPDR) is the earliest stage of diabetic eye disease. Microscopic changes occur in the blood vessels of the eye in NPDR. The changes typically do not produce symptoms and are not visible to the naked eye. This paper aims to investigate a method for distinguishing NPDR based on Electroretinogram (ERG).

Method: The ERG responses were recorded in 20 eyes from 14 patients with NPDR and 20 eyes from 20 healthy subjects as the control group. The responses of three standard stimuli were collected for both groups. Time-domain parameters, including amplitudes and implicit time, and a nonlinear criterion, were used to differentiate the groups.

Results: This study showed that implicit time and amplitude of b-wave in dark-adapted 10.0 ERG and amplitude and implicit time of light-adapted flicker 30 Hz could distinguish between controls and NPDR groups. Theta values obtained for dark-adapted 10.0 ERG (p=0.0019), light-adapted 3.0 ERG (p=0.0021), and light-adapted flicker 30 Hz (p=0.0023) had significant differences between the groups.

Conclusion: The proposed features have made it possible to distinguish between healthy and NPDR eyes. Choosing an appropriate method can effectively evaluate inner retinal dysfunction, especially in diabetic retinopathy.

1. Introduction

Diabetes is a common type of metabolic disease which is characterized by high blood glucose. Diabetes consists of type 1 or insulin-dependent diabetes, caused by a reduced insulin secretion rate, and type 2 or non-insulin-dependent diabetes, in which body cells do not respond to insulin adequately [1–2]. Hyperglycemia is the main feature of diabetes, and after a while, it causes vascular and neurological changes [3–5].

Diabetes has different complications, including cardiovascular disease, kidney, eye, brain, and nerve damages [6–10]. Diabetic retinopathy (DR) is the principal cause of vision loss and blindness among people with diabetes, especially working-age adults in developed countries [1, 11]. Intraretinal fluid accumulation and retinal hemorrhage leading to decreased vision are caused by diabetic retinopathy [12]. In the advanced stage of the disease, abnormal blood vessels proliferate on the retina's surface, may be associated with vitreous hemorrhage, fibrous proliferation, and traction retinal detachment [13].

Diabetic retinopathy consists of non-proliferative diabetic retinopathy (NPDR) and proliferative diabetic retinopathy (PDR). NPDR manifests by microaneurysms resulting in leakage of fluid and blood into the retina. PDR, which is characterized by neovascularization, is the more advanced DR [14–15].

Although DR involves several stages of severity, even very severe DR can be completely asymptomatic. If diagnosed, the disease can be improved with treatment. Therefore, early diagnosis of the DR is critical,

especially in the early stages. Fluorescein angiography, visual evoked potentials (EVP), and electroretinography are usually used to determine if the patient needs treatment [16–18]. These methods can provide a definitive study of the visual function and possibly destructive effects of diabetes on the visual system [19].

Electroretinogram (ERG) analysis is usually performed in the time-domain analysis. By measuring the two parameters of implicit time and amplitude of the waves, it is hard or impossible to detect minimal changes caused by NPDR. Biological signals like ERG are complex and have variable dynamics. Therefore, finding an appropriate method for processing these signals is very difficult. Processing methods attempt to extract the maximum information about the proper functioning or non-functioning of the related organs. Different signal processing methods have been applied to ERG, including time-domain, frequency-domain, and time-frequency domain analyses [20–26]. Besides, nonlinear features have been used to analyze the ERG [27–28].

This article intends to investigate the possibility of differentiating between normal and NDPR groups using a nonlinear feature.

2. Materials And Methods

2.1 Data description

The Ethics Committee at the Ophthalmic Research Center affiliated with Shahid Beheshti University of Medical Sciences Tehran, Iran, approved this study. The study included 20 eyes of 14 patients with NPDR and 20 eyes of 20 healthy subjects as the control group. The control subjects had no known visual system abnormalities, normal findings in the ophthalmic examination, and normal full-field ERG (ffERG). The mean±statndard deviation (SD) age of the NDPR patients and controls was 62.19±7.33 and 57.24 ±7.11 years, respectively.

The ERG signals were recorded using Roland Consult (Brandenburg, Germany) from both eyes simultaneously. Pupils were fully dilated using topical tropicamide 1%. Flashes of white light evoked the ERGs. The duration of the flash was 20 μs with the interstimulus interval of 1.5 seconds. After 20 minutes of dark adaptation the subjects put their head on Ganzfeld stimulator, and the dark-adapted 10.0 ERG were recorded. In the next step, photopic recordings were preceded after a light adaptation of 10 minutes to a background light of 30 cd/m^2.

The International Society for Clinical Electrophysiology of Vision (ISCEV) has been continuously standardizing different methods to achieve world-comparable responses [29]. The ISCEV standard full-field ERG [30] includes three responses of dark-adapted 10.0 ERG, light-adapted 3.0 ERG, and light-adapted 30 Hz flicker were considered in this study.

2.2 Feature Extraction

In recent years, different methods for ERG signal processing have been proposed with some advantages and disadvantages. However, the goal of all methods is to find the best way to analyze the ERG signals. The standard characteristics of ERG signals, which have been evaluated in most research, include ERG waves' amplitude and implicit time.

The ERG length is normally 200 milliseconds, and the first 80 milliseconds are the most critical part of the signal; because it contains the main components. Therefore, one of the fundamental challenges of processing ERG is its short length. Nonlinear methods could be the right choice in such signals to represent the signal's dynamic, which cannot be extracted through conventional methods.

2.2.1. Mapping Method

In this method, ERG is mapped to a parabolic curve. Therefore, the pairs of $\left(X_i, \left(\bar{X} - X_i\right)^2\right)$ are used to rearrange the points of ERG. The parabolic curve could provide a high resolution for distinguishing between different signals. The distribution of points in the parabolic curve is obtained through a two-degree polynomial equation as follow [28]:

$$Y = \alpha x^2 + \beta x + \gamma$$

1

The three main parameters of this equation are α, β, and γ. The distribution of points in a parabolic curve can have three states. The accumulation of points may be more to the left, right, or approximately divided into both sides equally. An illustration of the possible distribution of signal points on the axis is shown in Fig. 1.

The time series (ERG in our study) may include negative or positive amplitudes. Therefore, based on the $\left(X_i, \left(\bar{X} - X_i\right)^2\right)$,the square of the signal causes these parts of the signal to accumulate on the left or right side of the curve. In this way, we can even interpret the positive and negative amplitudes of ERG.

A criterion for measuring the distribution of points on the right or left side of the curve is the angles made by drawing a line from the beginning to endpoints distributed on the parabolic and horizontal axis. If the accumulation of points were on the parabolic curve's right, it indicates that the angle is less than 90 degrees. Such a result means the signal contains positive waves with higher amplitudes. On the other hand, if the accumulation of points were on the left of the parabolic curve, it leads to the angle, which is less than 90 degrees.

Negative angles confirm that signals contain negative waves with higher amplitudes. Signals with small angles (close to zero) indicate the balance between positive and negative waves [28]. The calculation of angles and measuring accumulated points on the curve's left or right side is shown in Fig. 2.

The tangent is defined as the ratio of the opposite side to the adjacent side. Theta is defined as the inverse of the tangent function, which is the angle whose tangent is a given number:

$$\theta = arctan\frac{opposite\,(aorb)}{adjacent}$$

2

In positive angles, the opposite side is "a," which is a portion of b-wave amplitude, and in the negative angle, the opposite side is "b," which is a portion of a-wave amplitude. In both cases, opposite sides contain more amplitudes than other parts of a-wave and b-wave [28].

There might be cases where several dispersed data far away from the rest of the points open the angle's arc and show a larger Theta. In principle, most of the points have accumulated elsewhere, and if the upper arc angle is considered to be the accumulation of those points, the Theta angle may be smaller. A density criterion can be a solution to this problem. The density of points in the Theta arc can be calculated and multiplied by the Theta angle. Therefore, the density criterion decreases if the accumulation of points is less and the angle is large. On the contrary, the higher the accumulation of points and the smaller the angle, the more robust the density criterion [28].

$$Density = \theta \times Numberofpointsinthearcof\theta$$

3

Figure 4 shows the different densities of points in the Theta angle arc for the two sample time series. As can be seen, Figure 3(a) shows the proportional distribution of points and the formation of a corresponding logical angle. However, in Figure (b), two points are located far from the concentration of points, making it a more significant angle. This false magnification of the angle can lead to misjudgment.

2.3. Statistical Analysis

The data do not have a normal distribution, and the two studied groups (healthy and NPDR eyes) are independent. Therefore, the Mann-Whitney U test was employed to reveal the significance of ERG features. Values are given as the mean ± standard deviation (SD), and the significance level is defined as $p < 0.05$. Moreover, the effect size statistic for the Mann-Whitney U test is “r” defined by the following formula:

$$r = \frac{Z}{\sqrt{N}}$$

4

where N is the total number of observations, and then runs the test SPSS reports the appropriate Z value. Effect sizes can be divided in four groups according to their r-values: "small" (0.1<|r|<0.3), "medium" (0.3<|r|<0.5) or "large" (|r|>0.5) [31].

3. Results

The time-domain method is known as the standard method of ERG analysis. A sample of ERG for healthy normal and NPDR is presented in Fig. 4. Therefore, the implicit time and amplitude of a- and b-waves for all individuals were presented in Table 1. A-wave amplitude did not show any significant difference ($p < 0.05$) in light-adapted 3.0 ERG.

Table 1
Time-domain characteristics of the non-proliferative diabetic and normal eyes

	Diabetic Retinopathy	Normal	P-Value	Z	r
Dark-adapted 10.0 a-wave			0.0201	2.1124	0.4236
Amplitude (μV)	23.24±9.12	59.11±12.33	0.0444	-1.0247	0.2056
Implicit time (ms)	39.44±5.76	29.12±4.12			
Dark-adapted 10.0 b-wave			0.0113	7.2587	1.5527
Amplitude (μV)	37.89±11.19	90.11±13.19	0.0488	-0.6668	0.1123
Implicit time (ms)	71.22±8.35	61.02±9.14			
Light-adapted 3.0 a-wave			0.0527	1.1022	0.2044
Amplitude (μV)	10.21±8.16	19.04±9.17	0.0475	-1.1918	0.2431
Implicit time (ms)	27.14±7.24	19.15±7.52			
Light-adapted 3.0 b-wave			0.0019	2.2147	0.4414
Amplitude (μV)	22.55±12.37	95.41±18.18	0.0402	-0.4512	0.1258
Implicit time (ms)	48.83±8.96	40.51±7.77			
Light-adapted Flicker 30 Hz			0.0185	1.4147	0.2758
Amplitude (μV)	50.17±5.67	68.02±7.11	0.0224	-0.4863	0.1180
Implicit time (ms)	40.42±7.16	34.75±5.23			

In the next step, the parabolic curve parameters (α, β, and γ) were calculated for all of the six ERG signals. The values obtained for the first parameter (α) were all the same for both groups. The other two parameters (β, and γ), which represent the parabolic width and its location on the vertical axis, had different values, but no significant changes were observed.

Theta angles for three studied stimuli are shown in Table 2. Theta values obtained for dark-adapted 10.0 ERG ($p = 0.0019$), light-adapted 3.0 ERG ($p = 0.0021$), and light-adapted flicker 30 Hz ($p = 0.0023$) had significant differences between the groups. Using the density criterion and its multiplication in the amount of Theta, we found a significant difference among dark-adapted 10.0 ERG ($p = 0.0012$), light-adapted 3.0 ERG ($p = 0.0013$), and light-adapted 30 Hz flicker ($p = 0.019$).

Table 2: The mean and standard deviation of Theta feature for non-proliferative diabetic retinopathy and the normal eyes in six ERG signals recorded with different stimulus

	Abnormal Eyes	Normal Eyes	P-Value of	P-Value of	Z	r
Dark-adapted 10.0	-8.11 2.23	-33.174.55	0.0019	0.0012	2.5436	0.5321
Light-adapted 3.0	22.19 7.16	50.366.87	0.0021	0.0013	2.6157	0.5411
Light-adapted Flicker 3.0	13.44 3.15	34.244.41	0.0023	0.0019	2.3734	0.5124

Figure 5 indicates an example of Theta angle in dark-adapted 3.0 ERG for (a) NPDR and (b) normal eyes. It can be seen that the value of the Theta angle in the NPDR eye has decreased compared to a normal eye.

4. Discussion

In this study, a nonlinear criterion was used to evaluate the ERG of NPDR and healthy eyes. This article aimed to investigate the ability of nonlinear features to differentiate the changes in eyes with NPDR compared with normal eyes.

ERG has valuable characteristics that can be used as an independent diagnostic method. Retinal function, retinal disease progression, or even control in some retinal diseases can be well assessed using an ERG signal. The ERG changes with some retinal diseases, such as retinitis pigmentosa (RP) or central retinal vein occlusion (CRVO), are so significant that their effects on implicit time and amplitude are apparent. However, in some cases or the early stages of the disease, little difference occurs with the normal state due to minimal changes in the ERG's amplitude and implicit time. However, these changes have led to changes in ERG dynamics and will undoubtedly be detectable using a sensitive feature to even small changes.

Various nonlinear features have been applied to ERG signals so far. These features include the Lyapunov exponent, Hurst exponent, approximate entropy, and fractal dimension. Nonlinear features have made a good distinction between healthy and abnormal groups [27]. Another feature that could show the dynamic of ERG in CRVO patients was mapping the ERG to a parabolic curve and extracting an angle criterion based on the arrangement of points on a new curve [28]. Due to the short length of the ERG,

geometric features or signal mapping can create a different point of view to the distribution of time series points, and perhaps the hidden dynamics of the signal can be detected.

NPDR has a more negligible effect on the ERG signal than the proliferative stage diabetic retinopathy. Therefore, in this study, we tried to investigate the potential of mapping features in this type of diabetes. Since the standard criteria for ERG analysis refer to the amplitude and implicit time of the ERG components, we compared the two groups with the time-domain characteristics before evaluating the nonlinear method. B-wave amplitudes were significantly lower in the NPDR group [32]. The b-wave amplitude is believed to be a good indicator of retinal circulation. Therefore, our results confirmed the insufficiency in the retinal circulation of the NPDR group.

The implicit times of the a- and b-wave were increased in the NPDR group. Previous research has also reported the delay in the a- and b-wave in various retinal diseases [33–34]. The increase in the implicit time in b-wave has already been confirmed in various retinal diseases [35–36]. It was reported that hat delays in the development of b-wave in patients with CRVO could manifest the disease progression and the occurrence of retinal neovascularization [36]. This similarity between the results and PDR nature, characterized by neovascularization, could be an essential point. It may help the ophthalmologists to early diagnose the progress of NPDR and its advance towards PDR.

In the Theta angle criterion, the accumulation of points on the right-hand side is somehow an indicator of the b-wave amplitude. Past studies have shown that if the ERG b-wave generated in the neural retinal layers becomes very small in the eye with CRVO, it can be concluded that the overall retinal ischemia is very severe [37–41]. The Theta angle of the NPDR group for dark-adapted 10.0 was negative and reduced dramatically in the NPDR group. A negative angle refers to the a-wave. So, it seems that bipolar cells are disrupted. In some NPDR patients, Theta-angle changes were smaller. This difference could be attributed to the severity of DR. This idea can be further explored by examining patients with PDR comparing the angle differences observed in this group with the non-proliferative group.

5. Conclusion

Although various imaging techniques have always been reliable to diagnose retinal diseases and monitor their progression, such methods are also more expensive than a signal recording method. The nonlinear criterion evaluated in this study showed that selecting the appropriate feature to extract the ERG signal dynamics can increase the chance of detection and more accurate investigations based on this signal.

The Theta criterion can be a practical feature for diagnosing DR, and it can be a valuable method in other retinal diseases. This criterion provided helpful information about photoreceptors and different layers of the retina.

In this study, we examined the ERG signals of NPDR patients. It is suggested that Theta can be used to evaluate other types of diabetic retinopathy.

List Of Abbreviations

CRVO: Central Retinal Vein Occlusion; **DR:** Diabetic Retinopathy; **ERG:** Electroretinogram; **EVP:** Visual Evoked Potentials; **ISCEV:** Clinical Electrophysiology of Vision; **NPDR**: Non-Proliferative Diabetic Retinopathy; **PDR**: Proliferative Diabetic Retinopathy; **RP:** Retinitis Pigmentosa; **SD:** Standard Deviation;

Declarations

Acknowledgments

We are grateful to the Ophthalmic Research Center of Shahid Beheshti University for collaborating on classifying and reviewing patients' clinical information and monitoring database registration. We would also like to thank Dr. Sare Safi for coordinating with patients and recording the ERG signals.

Funding: Ophthalmology Research Center of Shahid Beheshti University funded this work.

Conflict of interest: The authors declare that they have no conflict of interest.

Ethical approval: All procedures performed in studies involving human participants were by the ethical standards of the (Ethics Committee of Ophthalmic Research Center, Shahid Beheshti Medical University (Tehran, Iran)) and 1964 Helsinki declaration and its later amendments or comparable ethical standards.

Consent to participate: Informed consent was obtained from all individual participants included in the study.

Availability of data and material: The data is private.

Code availability: The codes are not public.

Authors' contributions: Zahra Maleki (writing the paper, data analysis), Soroor Behbahani (Supervisor, data analysis, review of the paper), Narsis Daftarian (Advisor, Subjects analysis, review the paper)

References

1. American Diabetes Association. Diagnosis, and classification of diabetes mellitus. Diabetes Care. 2009;32*((*Suppl 1*):*):62–7.
2. Pescosolido N, Buomprisco G. Psychophysical exams as early indicators of diabetic retinopathy. Eur Endocrinol 2014; 10*(1)*: 61–65.
3. Bornstein J. Lawrence RD. Two types of diabetes mellitus with and without available plasma insulin. Br Med J. 1951; 7*(*4709*)*: 732.
4. Sima AAF. Sugimoto K. Experimental diabetic neuropathy: an update. Diabetologia 1999; 42: 773–78.

5. Irvine WJ, Holton DE, Clarke BF, Toft AD, Prescott RJ, Duncan LJP. Familial studies of type- I and type-II idiopathic diabetes mellitus. Lancet 1977; 310*(*8033*)*: 325–328.
6. Low Wang CC. Hess CN, Hiatt WR. Goldfine AB. Atherosclerotic cardiovascular disease and heart failure in type 2 diabetes mechanisms, management, and clinical considerations. Circulation 2016; 133*(*24*)*: 2459–502.
7. Ravenscroft, Eleanor F. Diabetes and kidney failure: How individuals with diabetes experience kidney failure. Nephrology Nursing Journal 2005; 32*(*5*)*: 502–510.
8. Ewing DJ. Clarke BF. Diagnosis and management of diabetic autonomic neuropathy. Br Med J (Clin Res Ed). 1982; 285*(*6346*)*: 916–8.
9. Yang JK. Wang YY, Liu C. Shi TT, Lu L. Cao X, Yang FY. Feng JP, Chen C. Ji LN, Xu A. Proteome specific for eye damage can predict kidney damage in patients with type 2 diabetes: A case-control and a 5.3-year prospective cohort study. Diabetes Care 2017; 40*(*2*)*: 253–60.
10. Ryan M. Diabetes and brain damage: more (or less) than meets the eye? Diabetologia. 2006;49:2229–33.
11. Zheng Y. He M, Congdon N. The worldwide epidemic of diabetic retinopathy. Indian J Ophthalmol. 2012; 60*(*5*)*: 428–31.
12. Arora M. Pandey M, *Deep neural network for diabetic retinopathy detection. International Conference on Machine Learning* 2019; *189–193.*.
13. Crawford TN. Alfaro DV, Kerrison JB. Jablon EP. Diabetic retinopathy and angiogenesis. Current Diabetes Reviews 2009; 5*(*1*)*: 8–13.
14. Wang W, Lo ACY. Diabetic retinopathy: Pathophysiology and treatments. Int J Mol Sci. 2018; 19(6): 1816.
15. Viswanath K, McGavin DDM. Diabetic retinopathy: Clinical findings and management. Community Eye Health 2003; 16(46): 21–24.
16. Lee R. Wong TY, Sabanayagam C. Epidemiology of diabetic retinopathy, diabetic macular edema, and related vision loss. Eye Vis (Lond) 2015; 2: 17.
17. Heravian J. Ehyaei A, Shoeibi N. Azimi A, Ostadi-Moghaddam H. Yekta AA, Khoshsima MJ. Esmaily H. Pattern visual evoked potentials in patients with type II diabetes mellitus. J Ophthalmic Vis Res. 2012; 7*(*3*)*: 225–30.
18. Tzekov Y. Arden GB. The electroretinogram in diabetic retinopathy. Surv Ophthalmo.1999; 44*(*1*)*: 53–60.
19. Pescosolido N. Barbato A, Stefanucci A. Buomprisco G. *Role of electrophysiology in the early diagnosis and follow-up of diabetic retinopathy. Journal of Diabetes Research* 2015; *2018:8.*.
20. Barraco R. Bellamonte L, Brai M. *Time-frequency behavior of the a-wave of the human electroretinogram. In Proceedings of IFMBE, Palermo* 2007; *919–922.*.
21. Vilela C. Cortés V, Vallet M. Electroretinogram: technique and clinical applications. Rev Neurol. 1998; 26*(*151*)*: 444–7.

22. Bellomonte L. Barraco R. Brai M, Time-frequency behavior of the a-wave of the human electroretinogram. Medical Biomedical Engineering Computing 2007; 16: 919–22.
23. Ebdali S, Hashemi B, Jafarzadehpour E. Comparing the variation of time and frequency components of electroretinogram in patients with retinitis pigmentosa and healthy Individuals. J Mazandaran Univ Med Sci. 2017;26(145):110–21.
24. Miguel JM. Boquete L, Ortegaa S. Alén Cordero C, Bareaa R. Blancoc R. mfERG LAB: Software for processing multifocal electroretinography signals. Comput Methods Programs Biomed 2012; 108 *(1)*: 377–87.
25. Behbahani S, Ramezani A, Moridani MK, Sabbaghi H. Time-frequency analysis of photopic negative response in CRVO patients. Semin Ophthalmol. 2020; 35(3): 187–193.
26. Ahmadieh H, Behbahani S, Safi S. Continuous wavelet transform analysis of ERG in patients with diabetic retinopathy. Doc Ophthalmol. 2021; 142(3): 305–314.
27. Nair SS, Joseph KP. Chaotic analysis of the electroretinographic signal for diagnosis. BioMed Research International 2014b; Article ID 503920, 8 pages.
28. Sefandarmaz N. Behbahani S, Ramezani A. A novel method for electroretinogram assessment in patients with central retinal vein occlusion. Doc Ophthalmol. 2020; 140: 257–71.
29. Corici AC. Alexandru DO, Corîci OM. Puianu M, Iancău M. Ştefănescu-Dima A.Variability of normal values of electroretinogram Parameters Due to Aging in Healthy Individuals, Curr Health Sci J. 2015; 41*(1)*: 29–34.
30. Marmor MF. Fulton AB, Holder GE. Miyake Y, Brigell M. Bach M. ISCEV Standard for full-field clinical electroretinography. Doc Ophthalmol. 2009; 188:69–77.
31. Fritz CO, Morris PE, Richler JJ. Effect size estimates: Current use, calculations, and interpretation. J Exp Psychol Gen. 2012;141:2–18.
32. Kahn HA. Hiller R. Blindness caused by diabetic retinopathy 1974; 78*(1)*: 58–67.
33. Qiu H, Fujiwara E, Liu M, Lam BL, Hamasaki DI. Evidence that a-wave latency of the electroretinogram is determined solely by photoreceptors. Jpn J Ophthalmol. 2002;46:426–32.
34. Strom TM, Nyakatura G, Apfelstedt-Sylla E, et al. An L-type calcium-channel gene mutated in incomplete X-linked congenital stationary night blindness. Nat Genet. 1998;19:260–3.
35. Kjeka O, Bredrup C, Krohn J. Photopic 30 Hz flicker electroretinography predicts ocular neovascularization in central retinal vein occlusion. Acta Ophthalmol Scand. 2007;85:640–3.
36. Moschos M, Brouzas D, Moschou M, Theodossiadis G. The a- and b-wave latencies as a prognostic indicator of neovascularization in central retinal vein occlusion. Doc Ophthalmol. 1999; 99(2): 123–33.
37. Matsui Y, Katsumi O, Sakaue H, Hirose T. Electroretinogram b/a wave ratio improvement in central retinal vein obstruction. Br J Ophthalmol. 1994;78:191–8.
38. Breton ME, Schueller AW, Montzka DP. Electroretinogram b-wave implicit time and b/a wave ratio as a function of intensity in central retinal vein occlusion. Ophthalmology 1991; 98(12): 1845–1853.

39. Williamson TH, Keating D, Bradnam M. Electroretinography of central retinal vein occlusion under scotopic and photopic conditions: What to measure? Acta Ophtalmologica Scandinavica 1997; 48–53.
40. Yasuda S, Kachi S, Kondo M, Ushida H, Uetani R, Terui T, Piao CH, H Terasaki. Significant correlation between electroretinogram parameters and ocular vascular endothelial growth factor concentration in central retinal vein occlusion eyes. Investigative Ophthalmology & Visual Science 2011; 52: 5737–5742.
41. Sabates R, Hirose T, McMeel JM. Electroretinography in the prognosis and classification of central retinal vein occlusion. Arch Ophthalmol. 1983; 101(2): 232–235.

Figures

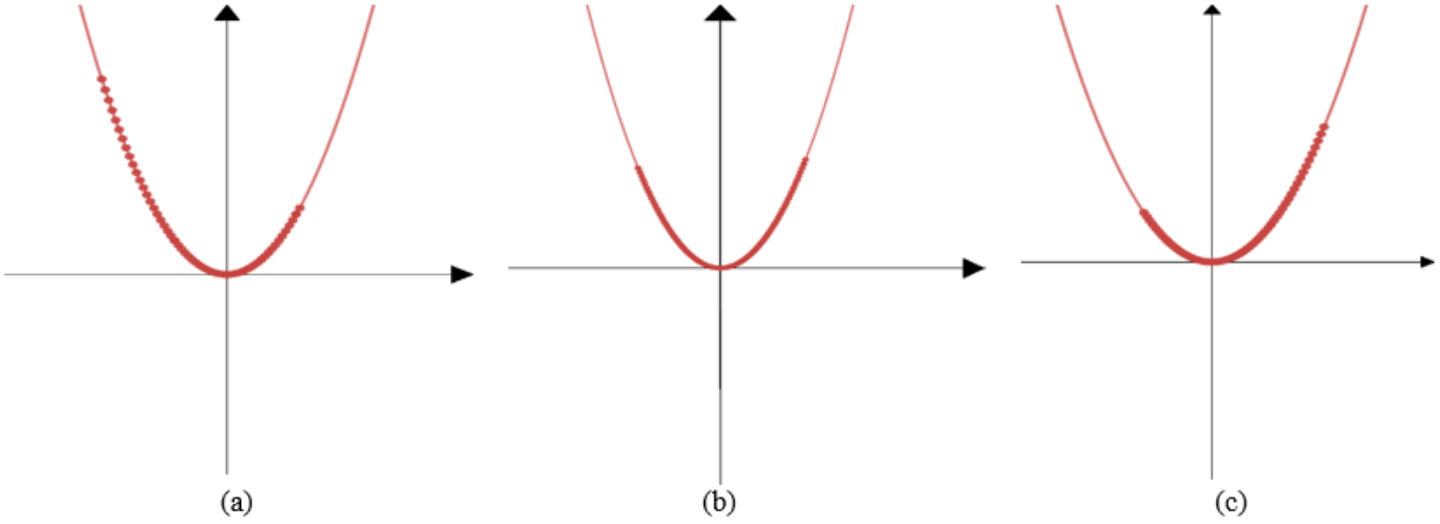

Figure 1

Three possible distribution of points on the parabolic curves fitted on an ERG signal; (a) accumulation on the left side, (b) equal distribution, and (c) accumulation on the right side of the curve

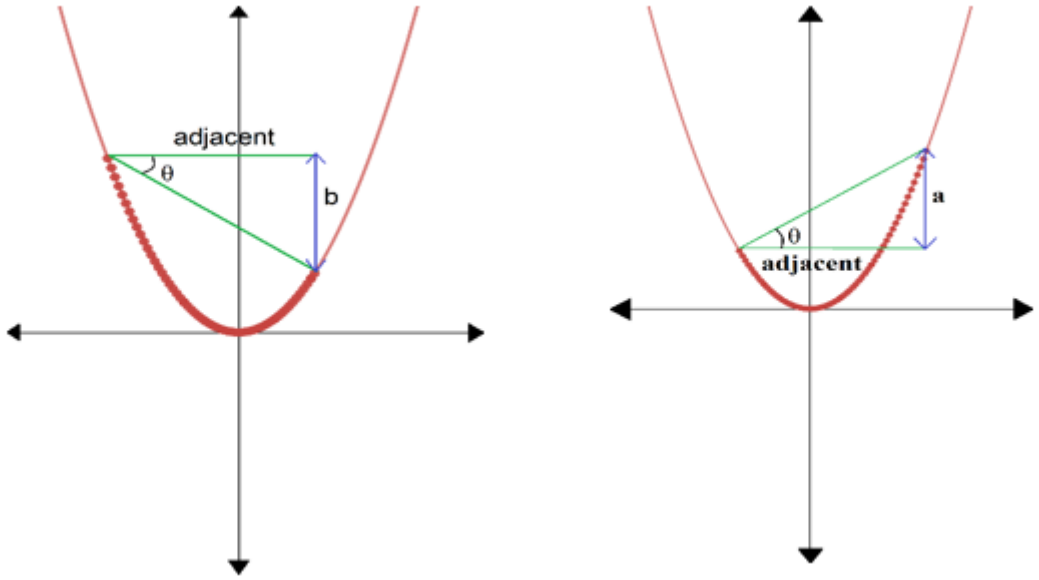

Figure 2

Positive and negative angle index in the parabolic map

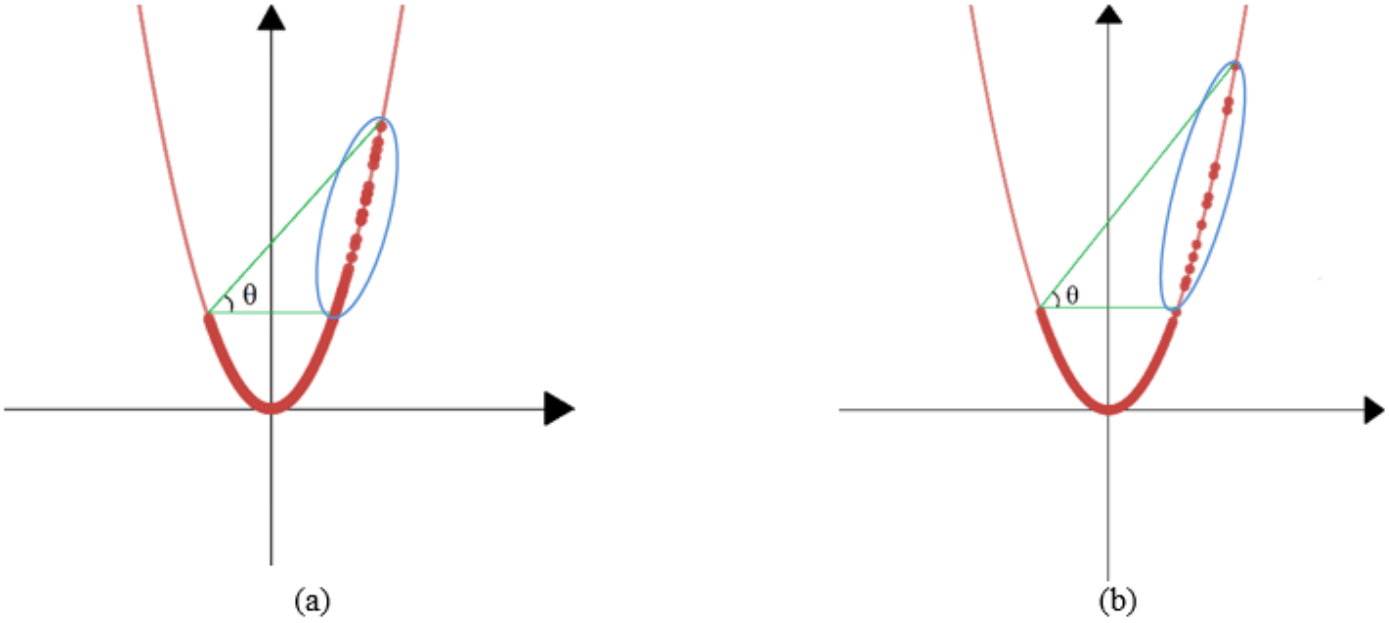

Figure 3

The density of points in the arc of Theta angle

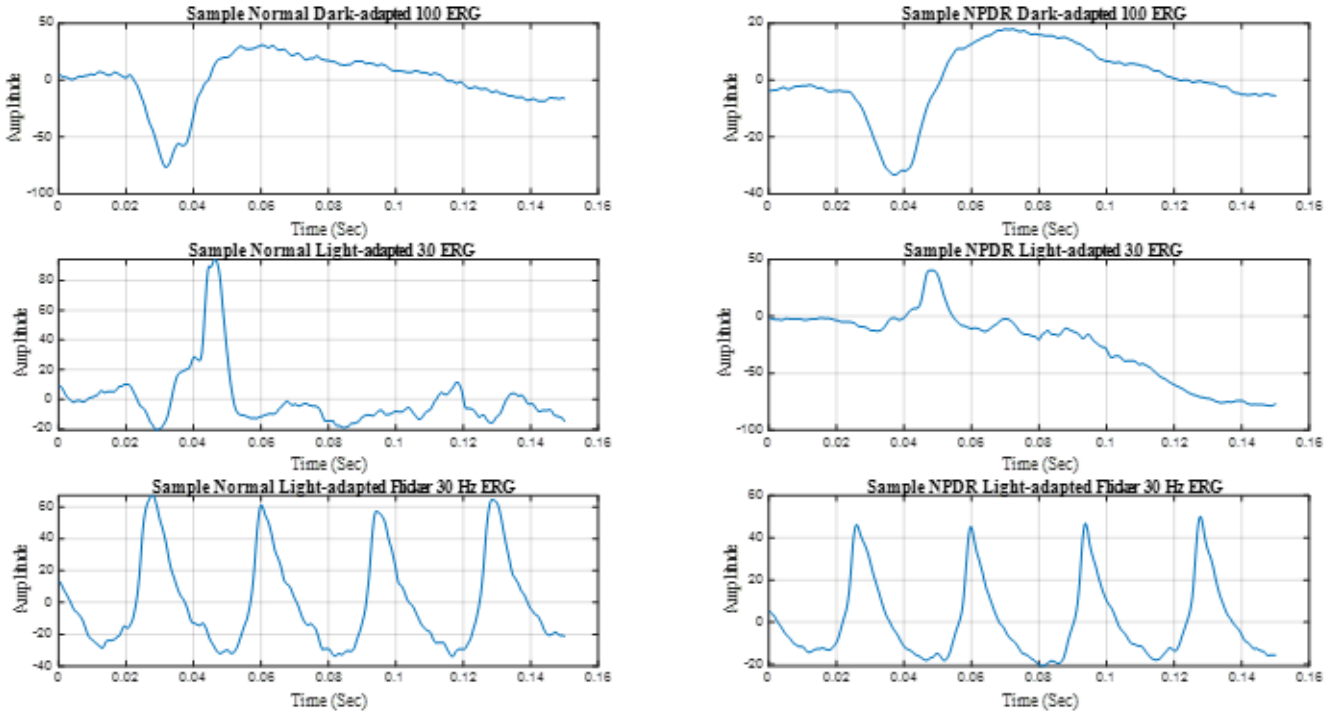

Figure 4

Sample healthy normal (column left) and non-proliferative diabetic retinopathy (column right) ERG for dark-adapted 10.0 light-adapted 3.0, and flicker 30 Hz, respectively.

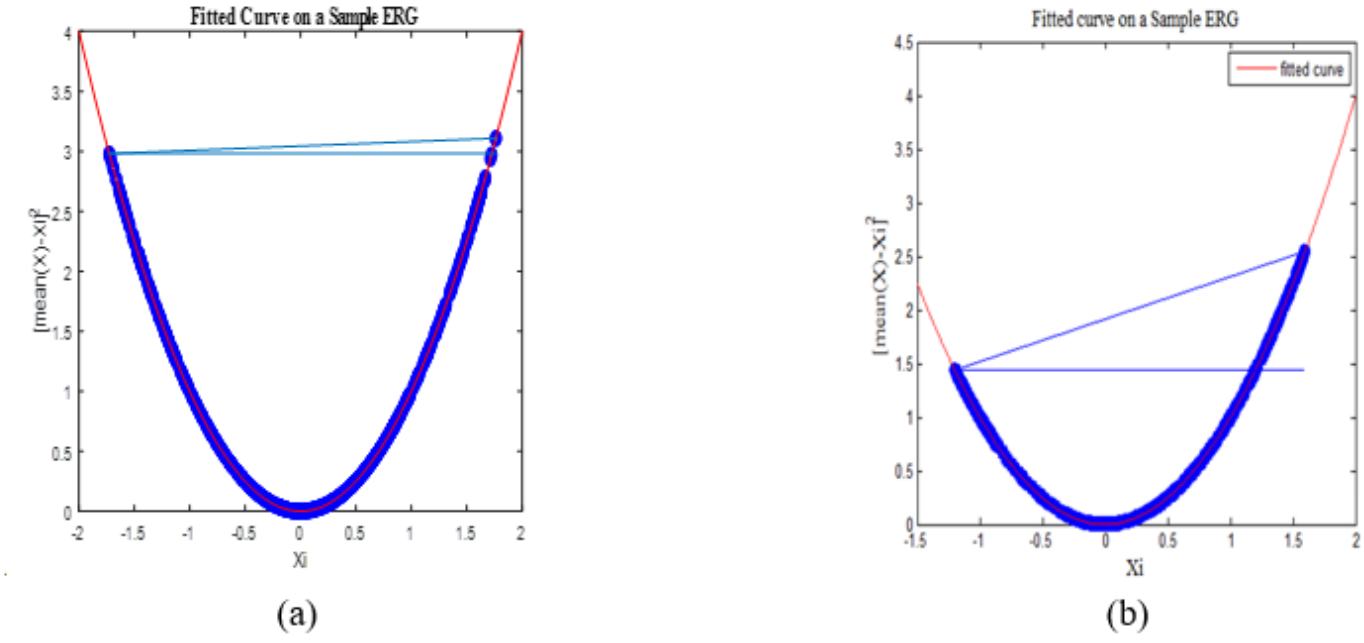

Figure 5

(a) Theta value obtained for a sample non-proliferative diabetic retinopathy; (b) Theta value obtained for a normal sample eye in dark-adapted 3.0 ERG